Q. J. R. Meteorol. Soc. (1989), **115**, pp. 965–981 551.558.21(941)

Airflow over a two-dimensional escarpment. I: Observations

By R. O. PITTS and T. J. LYONS

Environmental Science, School of Biological and Environmental Sciences, Murdoch University, Murdoch, W.A. 6150, Australia

(Received 7 October 1987; revised 26 October 1988)

SUMMARY

Observations of forced flow over the highly asymmetric topography of the Darling Scarp, Western Australia, are presented. These are typified by shallow surface gradient winds of 10–20 m s^{-1} with an inherent critical level aloft and a stable layer produced through nocturnal radiational cooling. The observations highlight a topographically induced hydraulic jump, lee waves or vertically propagating hydrostatic waves depending on the upwind stability and wind profile. The vertically propagating waves and hydraulic jump are observed to produce accelerated flow down the escarpment.

1. INTRODUCTION

Topographically induced waves have been observed by Lilly and Zipser (1972), Hoinka (1985) and Smith (1987), modelled by Peltier and Clark (1979), Clark and Peltier (1984), Klemp and Lilly (1975), Smith (1985), Durran (1986) and Tomine (1987), amongst others, and reviewed by Smith (1979). In particular, Smith (1979) suggests that when the forcing width of the topography is much larger than the length of a buoyancy oscillation, vertically propagating hydrostatic waves are formed that tilt upstream and create maximum wind speeds on the lee slope. Klemp and Lilly (1975) suggested from their linear study that the partial downward reflection of upward-propagating wave energy from the tropopause was responsible for this amplification of wind speed. However, Peltier and Clark (1979), using a nonlinear model, argued that it is caused by the downward reflection of wave energy from breaking waves at any level in the atmosphere, thus implying that wave overturning induces a critical level, leading to the reflection of wave energy at that level. The relative importance of these distinct mechanisms was argued on the basis of the modelling strategies employed (Lilly and Klemp 1980; Peltier and Clark 1980).

Windstorm events have also been described in terms of hydraulic flow and a subsequent jump (Vergeiner and Lilly 1970; Durran 1986). For this to occur, classical hydraulic theory requires a two-layered fluid, with a discontinuity between layers and a mechanism to prevent the vertical propagation of energy. Although Klemp and Lilly (1975) argued that such conditions were restrictive and not found in the atmosphere, Durran (1986) has suggested that the Boulder windstorm (Lilly and Zipser 1972) developed through an initial stage of a hydraulic jump, and Smith (1987) has observed atmospheric features that in his view are best described by a hydraulic jump.

Smith (1985) and Smith and Sun (1987) suggest that a two-layered fluid is not required for a hydraulic jump. The key element in their model is the decoupling of the low-level accelerated flow from the undisturbed flow aloft by a slow moving neutral region of variable depth. Durran and Klemp (1987) argue that wave overturning effectively induces a critical level, leading to a hydraulic jump.

Lilly and Klemp (1979) have also shown that terrain shape plays an important role in the creation of these flows. In particular, they showed that wave amplitude and wave drag were significantly enhanced for a ridge with gentle windward and steep leeward slopes in contrast to symmetrical terrain. Asymmetric terrain should also induce overturning at 0·5 times the vertical wavelength, instead of the 0·75 of symmetric terrain (Lilly and Klemp 1979).

This paper presents initial observations of flow over the Darling Scarp, near Perth, Western Australia. This escarpment is subjected to strong persistent synoptic winds and characterized by gentle windward and steep leeward slopes. All the data were collected under conditions expected to lead to topographically induced waves and illustrate the role of different mechanisms in the amplification of wind speed. A subsequent paper will address the modelling of these flows.

2. Climate and topography

Perth, with a population of one million, lies at approximately 32°S 116°E on a coastal plain in the south-west corner of Australia. The metropolitan area is adjacent to an almost straight north–south coastline and covers a relatively featureless sandy coastal plain. This plain has some low hills to the north of the city and the shallow estuarian valleys of the Swan and Canning rivers which originate in the 300 m-high Darling Scarp, along the eastern edge of the plain, about 25 km from the coast (see Fig. 1). The Darling Scarp, which descends to the plain in 3–5 km, marks the western edge of an extensive inland plateau and stretches for approximately 200 km in a north–south direction. Following Lilly and Klemp (1979), the western side of the scarp can be approximated to a half width of 1·6 km, whereas the eastern side is essentially flat. Drainage of the plain is poor and the water table is either at or close to the surface, leading to numerous shallow lakes. Apart from these, the plain is essentially flat.

During summer, synoptic winds above Perth are governed by the position of a subtropical ridge, which, combined with the formation of a heat trough down the coast, commonly results in shallow easterly surface gradient winds of 10–20 m s^{-1}. As mountains with gentle windward and steep leeward slopes significantly enhance mountain waves (Lilly and Klemp 1979), these are ideal synoptic conditions for the establishment of topographically induced waves under thermodynamically stable atmospheric conditions.

3. Data collection

The observational study of airflow over the escarpment centred on the collection of temperature profiles from an instrumented aircraft, following a west–east transect from the coast at Becher Point, to several kilometres east of the scarp (see Fig. 1). This transect was chosen as being the closest transect to Perth on which low-level flights were possible, as well as being removed from the majority of Perth's controlled airspace. The aircraft data were collected by a single-engine aircraft (either Cessna 182, Cessna 172 or Grumman) fitted with temperature, humidity and turbulence probes, and were supplemented by observations from the standard radiosonde release at Perth airport (Guildford), as well as Dines anemometer records taken at Jandakot and Perth airports and Pearce airforce base. As the nearest upstream radiosonde station is located at Kalgoorlie, some 550 km to the east, it was not possible to obtain a representative upwind undisturbed wind profile.

Air temperature was measured from the aircraft using a thermocouple fixed in a 20 cm aluminium housing, mounted on the underside of the wing. The housing shielded the probe from radiational effects but also introduced an adiabatic heating, as it brought the air partially to rest. Extensive tests at different airspeeds, in level flight, showed that this adiabatic heating could be represented as $dT = 0{\cdot}8(0{\cdot}01v)^2$, where dT is the increase in temperature from adiabatic heating, and v is the true air speed in knots.

The time response of the temperature probe was found to be made up of an initial fast response of the thermocouple plus a much slower response resulting from the thermal

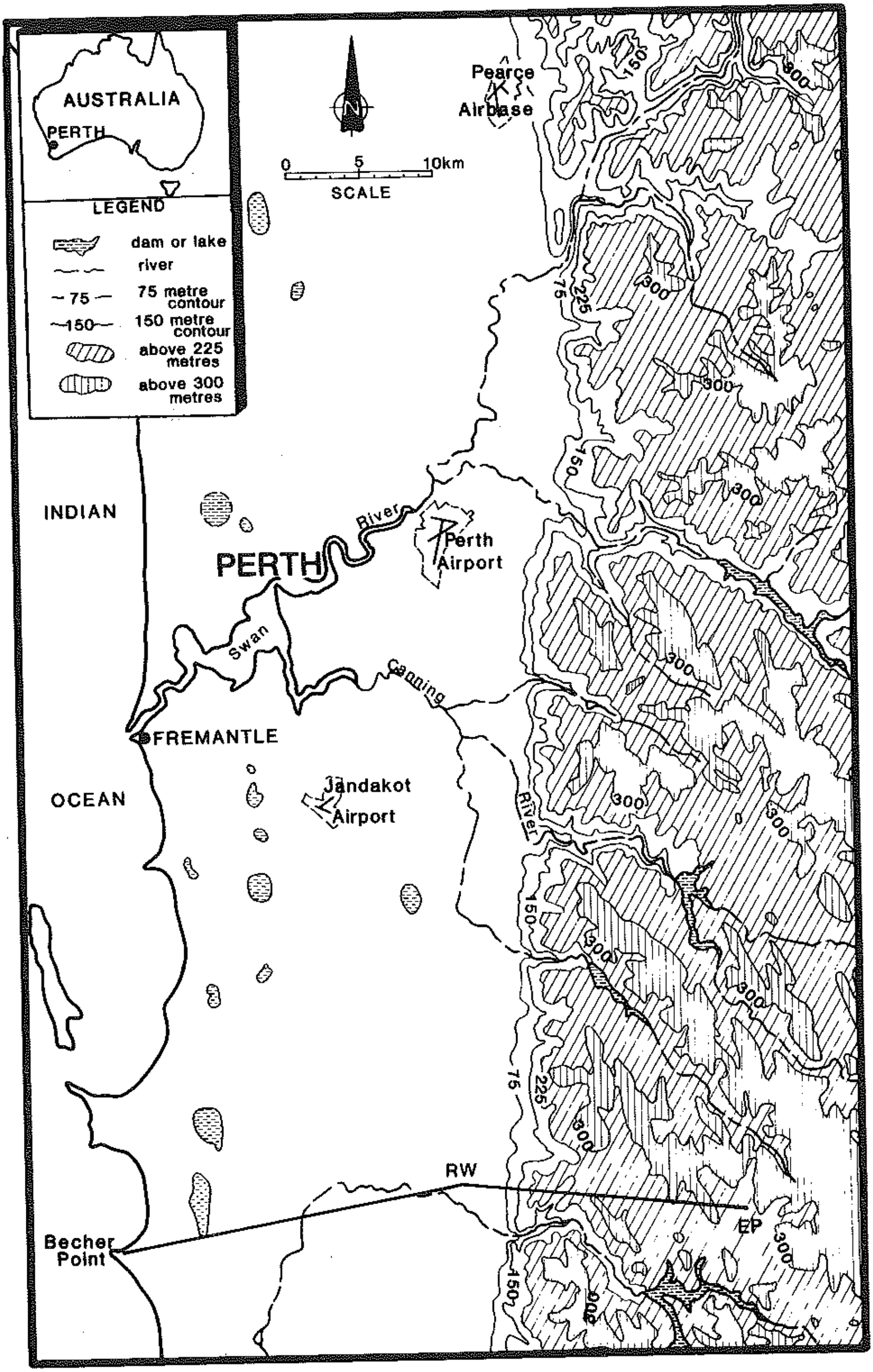

Figure 1. The Perth region, showing location of aircraft transect and fixed obsevations. EP marks the easternmost point of the traverse, whereas RW is the location of the closest aircraft profile to the escarpment.

inertia of the mounting. Such a response was modelled by representing the temperature change of the system as

$$dT_1/dt = (T_a - T_1)/t_1 + (T_2 - T_1)/r_1$$
$$dT_2/dt = (T_a - T_2)/t_2 - (T_2 - T_1)/r_2$$

where T_1 is the temperature of the thermocouple probe, T_2 the temperature of the mounting, T_a the actual air temperature, t_1 the time constant of the thermocouple, t_2 the time constant of the mounting and r_1, r_2 the reciprocal thermal resistance to the flow of heat from mount to sensor and *vice versa.*

The time constants and thermal resistances were determined experimentally by exposing the probe and housing to step changes in temperature in a high-speed wind tunnel at typical aircraft speeds. In the field, air temperature was found by solving the differential equations for T_a, given the thermocouple temperature, T_1, and assuming an initial mounting temperature. Air temperatures were also corrected for adiabatic heating. This overall correction for air temperature was found to give a relative error of ±0·2 degC for a variety of airspeeds, atmospheric profiles and aircraft configurations.

Relative humidity was measured with a Väisälä HMP114Y sensor with an accuracy of ±2% and a time constant <5 s. The sensor was mounted in the cockpit air inlet, which essentially sampled environmental air instantaneously. A qualitative indication of turbulence was obtained with a Borgelt MB-1-AV variometer using air in the rear of the fuselage as the static source. As this instrument was only used for a qualitative indication of turbulence, no further calibration beyond the manufacturer's was attempted. The output of all instruments was recorded on a strip chart recorder and later digitized at discrete intervals for analysis.

All of the experimental runs were undertaken near sunrise, as the surface heat flux is minimal and a nearly constant temperature profile over the 2–3-hour flight could be expected. Observations at this time are also comparable with the morning (nominally 22 GMT (06 WST—local time)) radiosonde release and ensure that the nocturnal radiation inversion was at its strongest.

Data were collected on 7 days during the austral summer of 1985/86 and 9 days during the austral summer of 1986/87, when Perth was under the influence of strong synoptic easterlies. Results for four of these days are presented which are typical of the situations encountered.

4. Observations

(*a*) *13 December 1986*

The synoptic situation at 06 WST was dominated by an anticyclone situated to the south of Perth, directing a gradient wind of 17·7 m s^{-1} from 69° across Perth. This synoptic pattern remained stationary over the experimental period. The winds observed from the radiosonde are shown in Fig. 2(b), which illustrates a strong surface wind decreasing rapidly with height and turning through the north to an upper westerly at 2800 m. Such a synoptic situation is typical of summer, wherein an anticyclone to the south-east directs easterlies of between 1000–4000 m depth across Perth. These easterlies have invariably been heated by convective mixing over the desert to the east of Perth during the previous day. Consequently, the upstream conditions observed by the aircraft, Fig. 2(a), show an upper layer which is near adiabatic (lapse rate 0·0015 K m^{-1}) from the previous day's convective boundary layer, a radiational inversion near the surface and a turbulent mixed layer below this.

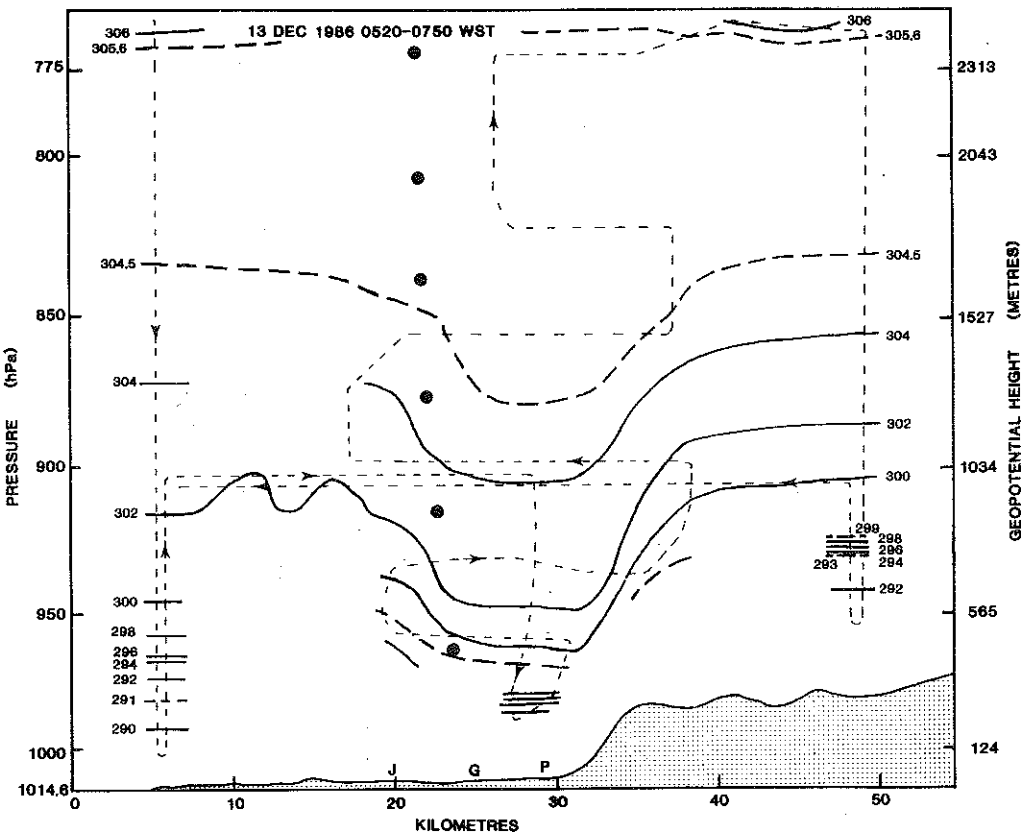

Figure 2(a). Cross-section of isentropes based on the aircraft observations for 13 December 1986. Large dots correspond to the approximate flight path of the radiosonde.

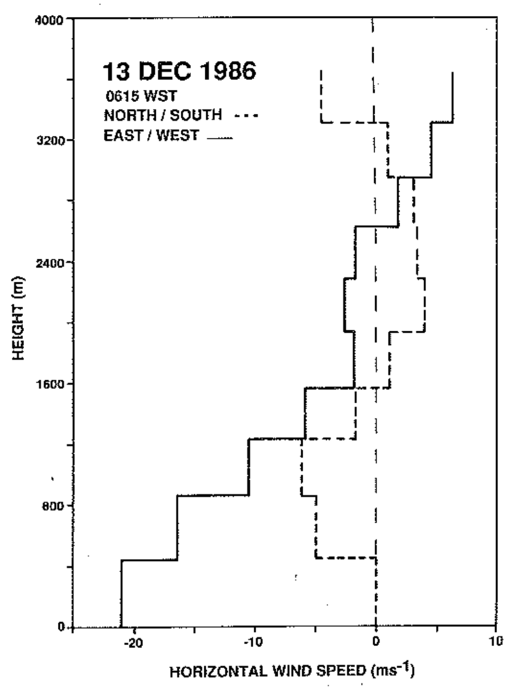

Figure 2(b). Guildford (Perth airport) radiosonde-observed horizontal wind speed profiles for 13 December 1986.

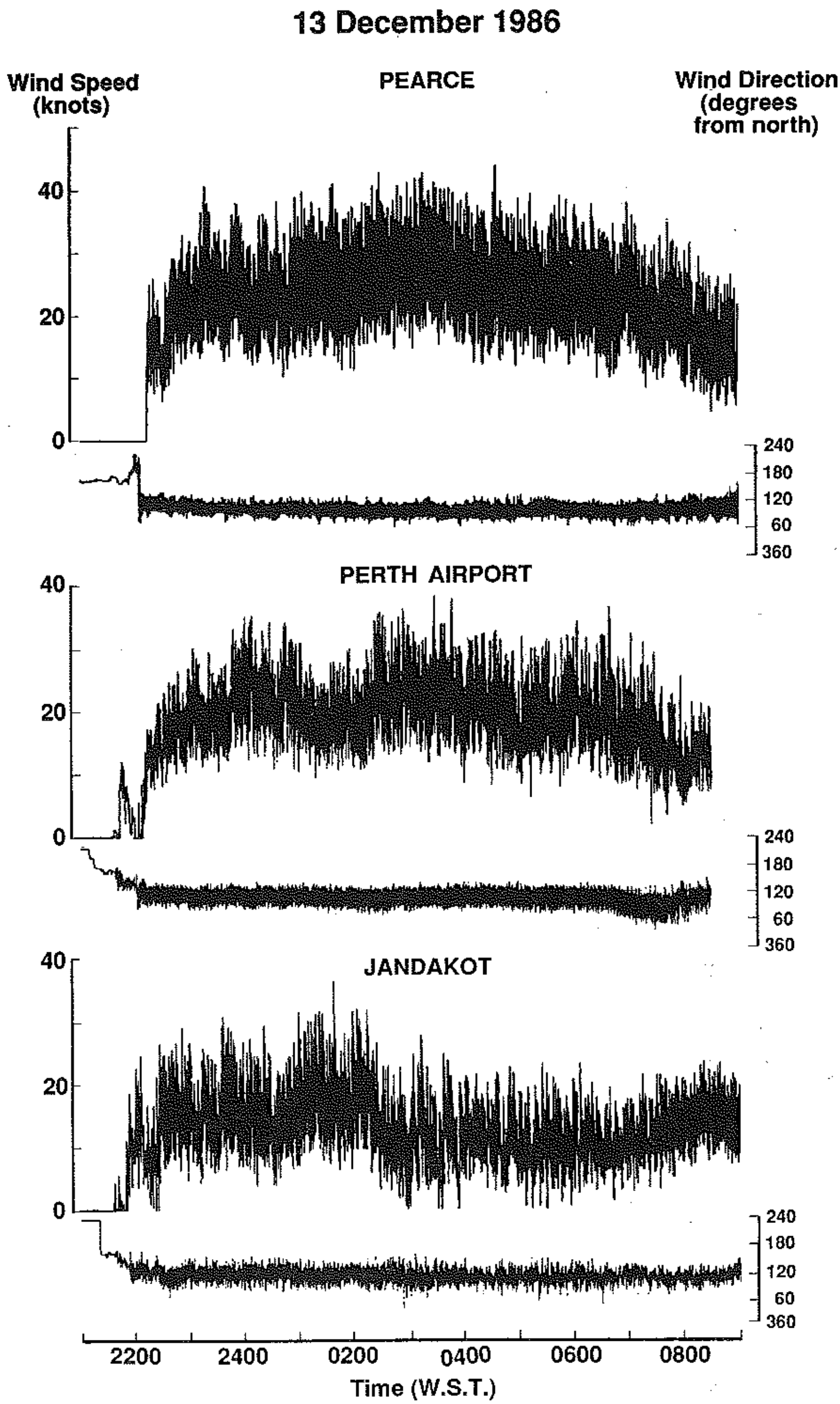

Figure 2(c). Anemometer traces from Pearce, Guildford and Jandakot for 13 December 1986.

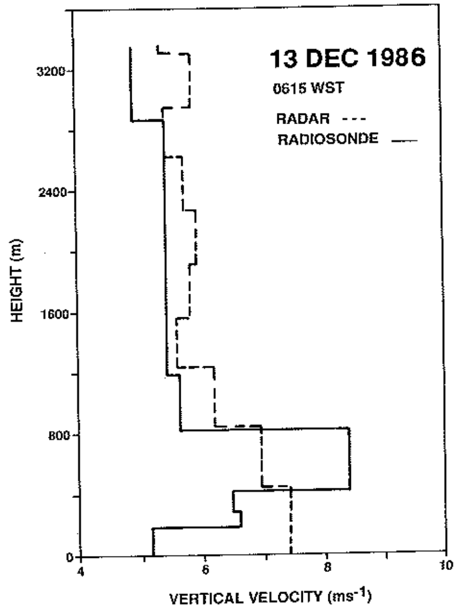

Figure 2(d). Computed vertical velocities experienced by the Guildford radiosonde for 13 December 1986 (following Corby (1957)).

As the flow moves over the escarpment, it produces a hydraulic-jump-like feature with a 9 km-wide trough and transient waves to the lee. In this trough, the top of the inversion (the 298 K isentrope) is about 270 m above ground level (a.g.l.) whereas at the top of the escarpment, it is approximately 500 m a.g.l. To the lee of the trough the inversion rises again to approximately 490 m a.g.l. This rise is associated with a region of mixing indicated by both turbulence and short-term (1–5 second) oscillations in the temperature and humidity traces. The overall effect of this mixing is evident in the downwind profile, which shows a broader, weaker inversion. Above the inversion, deviations in the isentropes slowly decrease until 2200 m, where there is no evidence of any vertically propagating waves.

Further evidence for this flow regime is provided by the anemometer traces, Fig. 2(c), which also illustrate the two-dimensionality of the flow. All traces illustrate a sudden onset of easterlies with the highest wind speed being recorded nearest the escarpment and marked changes in wind direction being observed furthest from the escarpment. This is in accord with the aircraft observations, which suggest that Pearce and Guildford anemometers would be in the shooting flow with high but constant wind speeds, whereas Jandakot should be in a turbulent lower-wind-speed regime downstream from the jump and thus characterized by increased fluctuations in direction.

Horizontal and vertical velocities experienced by the radiosonde and computed following the analysis of Corby (1957), are also in accord with the aircraft observations. The vertical velocity profile, Fig. 2(d), illustrates a 2–3 m s^{-1} increase in velocity above the average ascent rate of 5 m s^{-1} in the region 200–800 m. This is consistent with the jump region being just downstream of Guildford, and, as shown on Fig. 2(a), the radiosonde rising through the jump. The horizontal components show a maximum wind speed in the lowest 300 m, which is also consistent with Guildford being upwind of the jump and in the shooting flow.

(b) 21 January 1987

On this day, the synoptic situation was dominated by ex-tropical cyclone Connie situated 750 km north-east of Perth and a high pressure ridge to the south. These combined to produce a deep easterly flow over the region with a surface gradient wind of 15 m s^{-1} from 95° which slowly turned to a westerly at 5800 m (see Fig. 3(b)). Associated with this there was mid-level cloud at 3500 m and some cloud at 1000 m to the east of the observing area.

Figure 3(a) shows isentropes based on aircraft observations taken between 0520 and 0710 WST and illustrates a lee wave extending from the escarpment. This wave existed in the stable air above the rather deep (600 m) mechanically mixed layer, and appeared to have a maximum amplitude at 1000 m where its horizontal wavelength was approximately 4·6 km. At this level the aircraft experienced mean vertical velocities over 30 s of 2 m s^{-1}. At higher levels, the wave appears more complex and vertical velocities experienced by the aircraft were much less. Figure 3(c) shows the vertical velocities computed from the 0615 WST radiosonde, following Corby (1957), and these also illustrate velocities of 2 m s^{-1} extending from 1200 to 2400 m.

As it is not possible to determine precisely the amplitude of the lee wave from a single traverse through the wave system (Vergeiner and Lilly 1970), the analysis of Corby was followed, wherein the wave is assumed to be sinusoidal. This leads to an estimated amplitude of 102 m, or a trough-to-crest height of 204 m, which was used as a basis for determining the amplitude of the wave depicted in Fig. 3(a).

Although the wave pattern was stable over the 125 minutes of aircraft observations, it was not static. A traverse at 1000 m between 0715 and 0720 WST observed the wave out of phase with the original observations and with a slightly larger horizontal wavelength, being variable between 4·5 and 5·5 km.

(c) 3 February 1987

The synoptic situation was stationary with an anticyclone situated to the south and a trough extending down the coast, to produce a surface gradient wind of 15·6 m s^{-1} from 69°. Wind speed, observed by the radiosonde, increased to a layer average of 24 m s^{-1}, centred at 610 m, before decreasing rapidly to a layer-averaged zero easterly component in the layer between 1800 and 2100 m (see Fig. 4(b)).

Figure 4(a) shows the isentropes derived from the aircraft measurements, and these illustrate a strong vertically propagating wave that is tilted upstream. The wavelength can be estimated from the height of maximum streamline steepening, or assuming stationary conditions, isentrope steepening. Thus, Fig. 4(a) suggests a vertical wavelength of approximately 2300 m.

The wind profile observations suggest that the easterly component falls to zero at approximately 1900 m which corresponds to the inversion on the downwind side of the escarpment. Above the inversion the air is significantly drier than that below, implying that the upper air is from a different air mass and that the inversion is an interface between the two air masses. Thus, taking the inversion as corresponding to the height of zero easterly flow, Fig. 4(a) illustrates that it varies between 1900 and 2100 m across the observational area. Since the western edge is further from the disturbed region at this height, and for a wind reversal becomes the upwind source, the undisturbed critical level is at approximately 1900 m. This approximates 0·82 times the vertical wavelength, in which situation the theory of Clark and Peltier (1984) predicts resonant wave growth.

The anemometer traces, presented in Fig. 4(c), show that the Pearce anemometer, being closest to the escarpment, records the highest wind speeds, whereas the Guildford anemometer shows a more turbulent wind direction trace. The Jandakot instrument

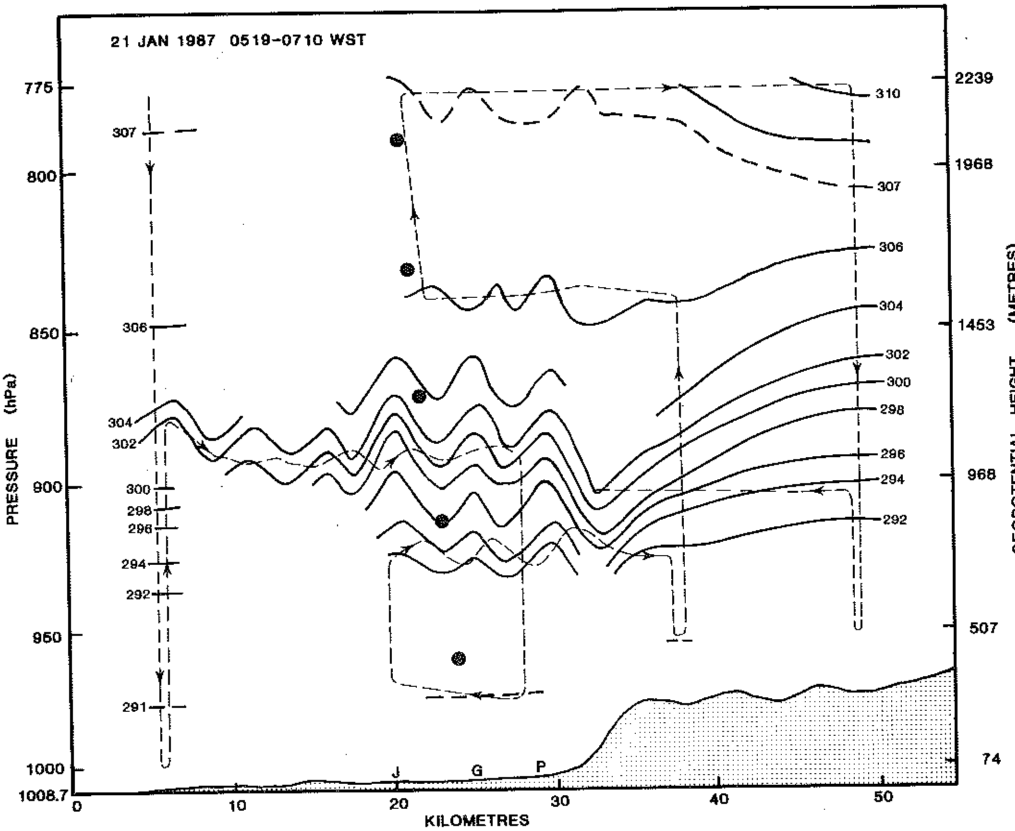

Figure 3(a). As Fig. 2(a) but for 21 January 1987.

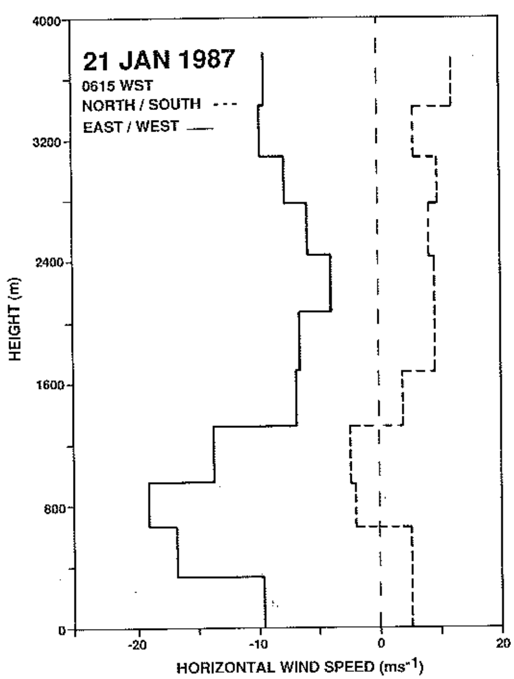

Figure 3(b). As Fig. 2(b) but for 21 January 1987.

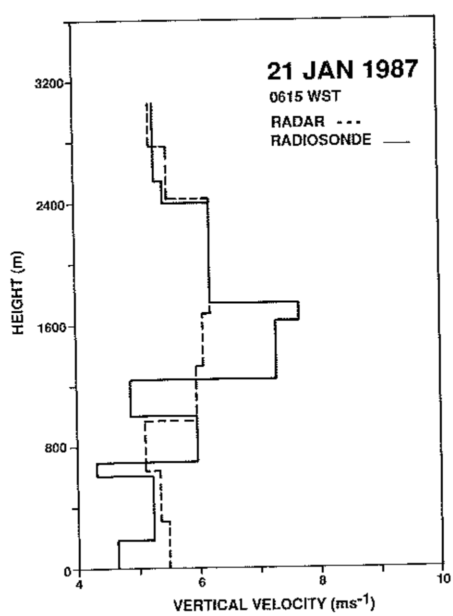

Figure 3(c). As Fig. 2(d) but for 21 January 1987.

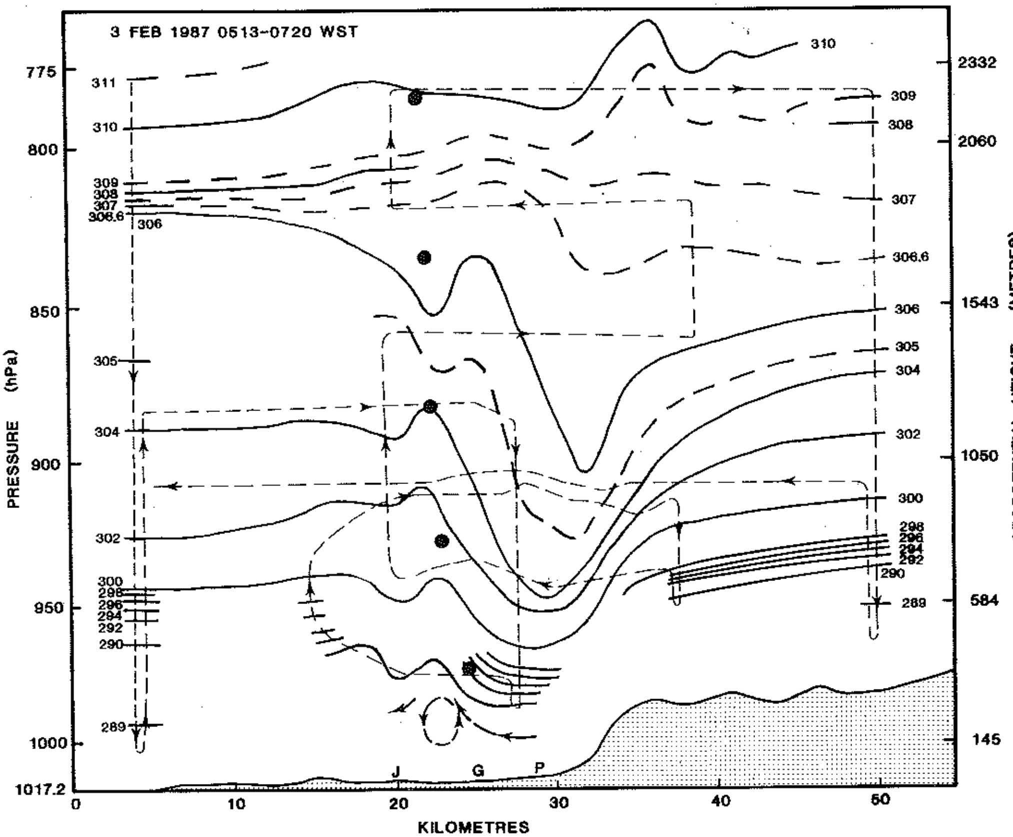

Figure 4(a). As Fig. 2(a) but for 3 February 1987.

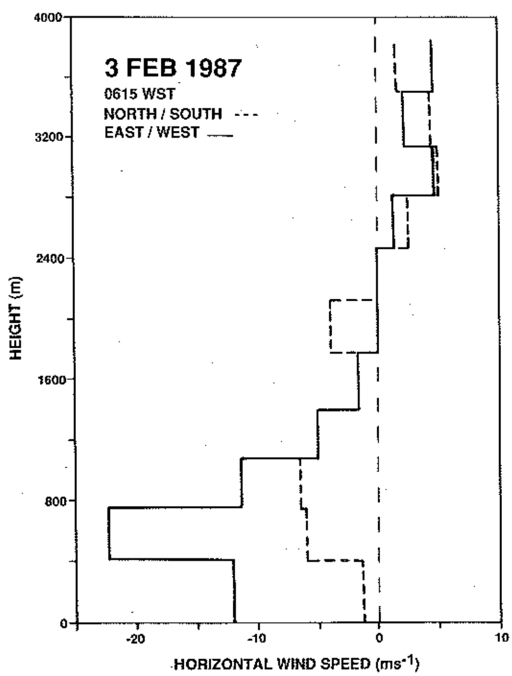

Figure 4(b). As Fig. 2(b) but for 3 February 1987.

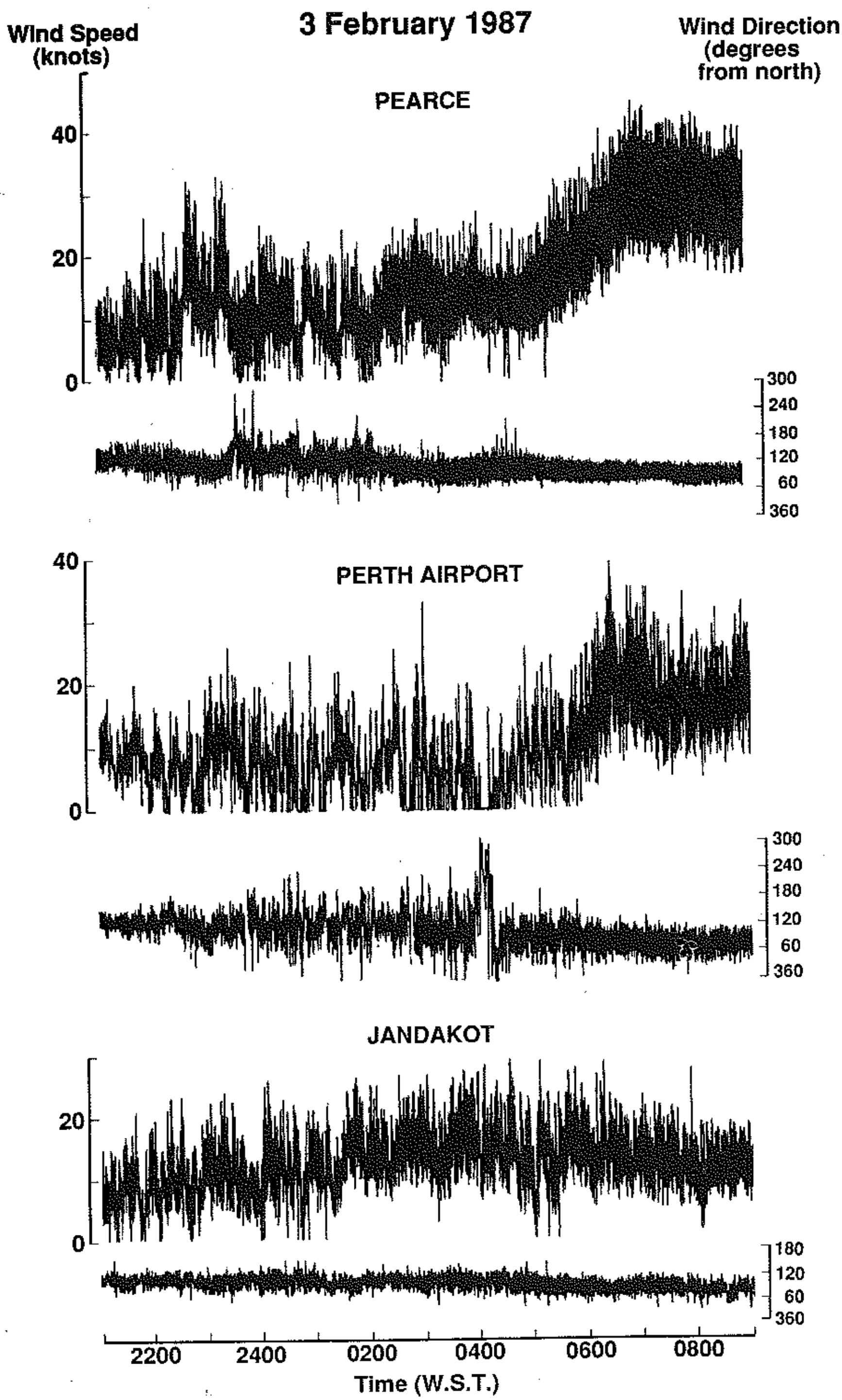

Figure 4(c). As Fig. 2(c) but for 3 February 1987.

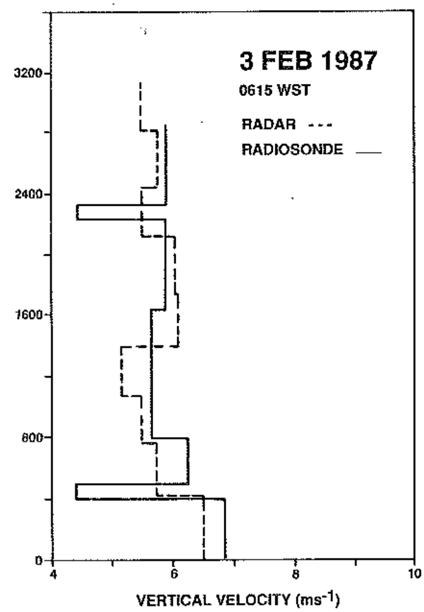

Figure 4(d). As Fig. 2(d) but for 3 February 1987.

recorded a much lower wind speed. This is consistent with Fig. 4(a), as Pearce is in the strong steady wind region, with Guildford at the edge of the area where the flow rebounds, and Jandakot away from the wave. Again, the horizontal separation of the anemometers (see Fig. 1) illustrates the north–south persistency of the winds and is consistent with the assumed two-dimensionality of the flow patterns.

Figure 4(c) shows that the wind increased substantially between 0530 and 0630 WST at Pearce and Guildford whilst remaining fairly constant or decreasing at Jandakot. This suggests a strengthening of the wave. The Guildford trace, between 0400 and 0530 WST, is indicative of a rotor in the region, as shown by the wind reversal, and the corresponding bursts of turbulence at Pearce during this period suggest that the rotor could lie on an east–west line between Pearce and Guildford. After 0530 WST, there is no evidence of a rotor on the anemometer traces, but the isentropic surfaces (Fig. 4(a)) suggest that the rotor is located to the lee of the wave trough, downwind of Guildford. This location of the rotor to the lee of the updraught region is consistent with the observations of Lester and Fingerhut (1974). Thus a strengthening of the wave leads to a widening of the wave trough and the possible movement of the rotor zone westward away from the escarpment.

Figure 4(d) illustrates vertical velocities of approximately $1{\cdot}5\ \mathrm{m\,s^{-1}}$ in the lowest 400 m above Guildford, slowly decreasing with height. This is consistent with the region of rise being above Guildford.

(*d*) *20 February 1987*

The synoptic conditions consisted of an anticyclone to the south-west and a trough along the coast, resulting in a temporary stable surface gradient wind of $17{\cdot}8\ \mathrm{m\,s^{-1}}$ from 85°. The 0615 WST radiosonde, Fig. 5(b), illustrates a strong easterly in the lowest 800 m, decreasing to zero at 1300 m, before increasing again with an easterly component of $5{\cdot}5\ \mathrm{m\,s^{-1}}$ at 2100 m and turning through south to a westerly at 2800 m.

Figure 5(a), based on aircraft observations between 0540 and 0750 WST, shows upstream conditions of a radiation inversion at 700–900 m above the mechanically mixed surface layer, with a stable layer above. On flowing over the escarpment, the inversion

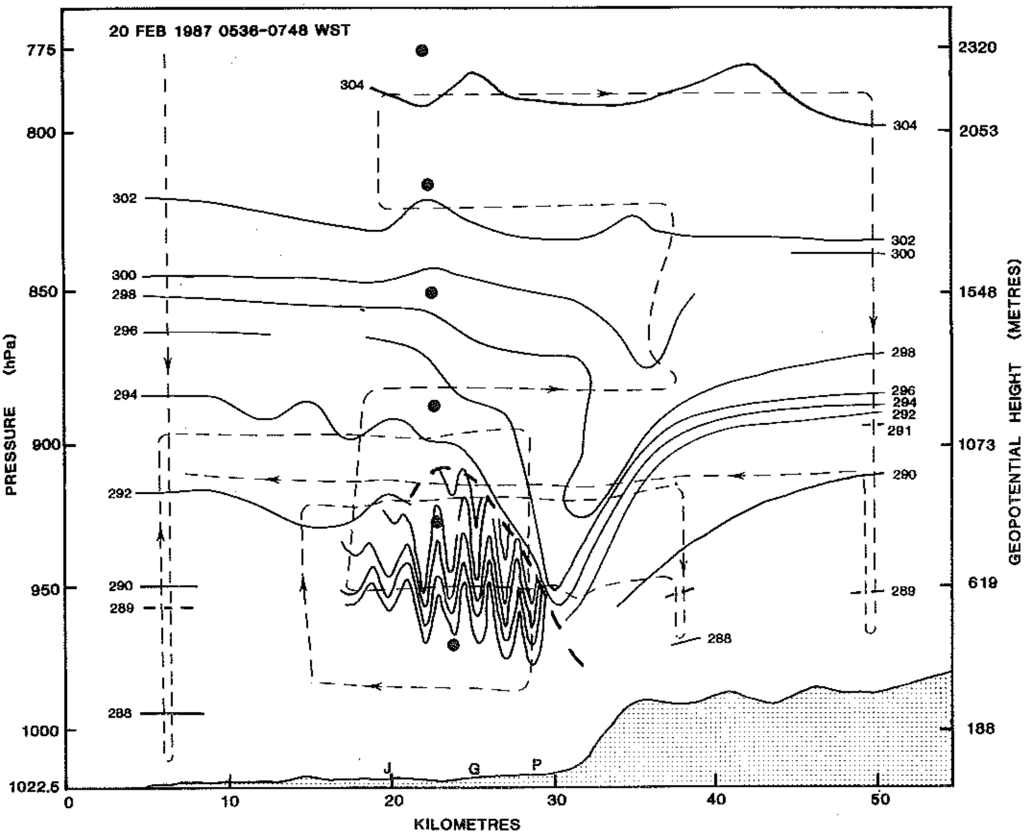

Figure 5(a). As Fig. 2(a) but for 20 February 1987.

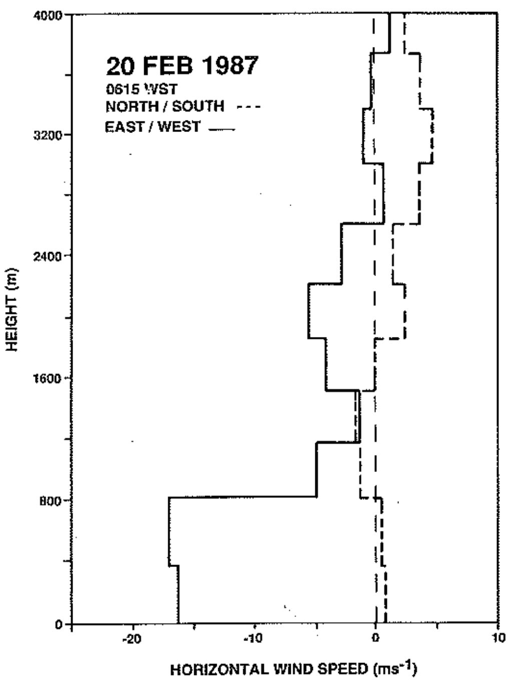

Figure 5(b). As Fig. 2(b) but for 20 February 1987.

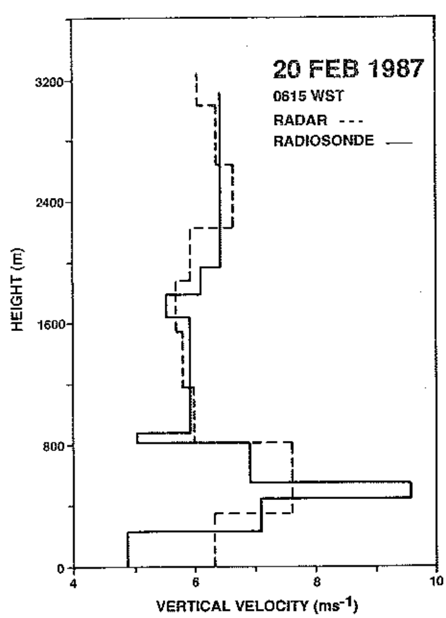

Figure 5(c). As Fig. 2(d) but for 20 February 1987.

descends 600 m, or twice the height of the escarpment. To the lee, two distinct flow regimes were observed. Below the dashed line of Fig. 5(a), a train of decreasing amplitude lee waves of horizontal wavelength 2·5 km was observed, whereas above the dashed line, the isentropes rebounded rapidly. A coherent picture between these regions was not possible because of the severe turbulence encountered.

Observations above the dashed line indicate wave overturning and show that the wave tilts markedly upstream. This overturning region was characterized by extreme turbulence, which suddenly stopped on the escarpment side. Above the height of overturning, there is little evidence of a vertically propagating wave. Below this the lee wave was also extremely turbulent. An indication of the severity of the turbulence can be seen in the marked mixing experienced by the inversion as the air moves away from the escarpment.

Further support for Fig. 5(a) can be seen in the radiosonde data (Fig. 5(b)), which shows a local minimum in horizontal wind speed in the overturning region. Although the sonde is 8 km from the escarpment, it appears to have passed through the perturbed flow where the wind would have little easterly component. Also the vertical velocities, Fig. 5(c), indicate a velocity of 3 m s^{-1} in the 200–800 m region, which is indicative of a strong wave.

5. Discussion

Smith (1979) defined topographically forced waves in terms of the mountain wavenumber, k, and the Scorer parameter, l, given by

$$l^2 = N^2/U^2 - U^{-1}(d^2U/dz^2)$$

where U is the wind speed and N the Brunt–Väisälä frequency. In particular, assuming that l is independent of height, $l^2 < k^2$ results in evanescent waves that are exponentially damped in the vertical, whereas with $l^2 > k^2$, strong buoyancy effects produce freely propagating waves. When l decreases with height, in such a way that $l^2 > k^2$ in the lower levels and $l^2 < k^2$ aloft, a trapped lee wave or resonance wave is produced (Smith 1979).

Real topography contains a spectrum of wavenumbers. Thus, most analytical studies have addressed bell-shaped hills where the maximum contribution to the energy spectrum occurs at $k = a^{-1}$, where a is the mountain half width (Klemp and Lilly 1980). In reviewing these, Smith (1979) noted the limiting cases of $al \ll 1$ for evanescent waves and $al \gg 1$ for propagating hydrostatic waves, and suggested that for $al \sim 1$, although buoyancy is still important and the flow can be considered hydrostatic, a dispersive trail of non-hydrostatic waves is formed.

The Scorer parameter is very sensitive to the second derivative of the wind speed, and noise from rawinsonde observations makes its determination difficult (Bower and Durran 1986). Hence most investigators, using observational data, neglect the curvature of the wind profile and approximate l^2 by N^2/U^2. Such an approximation reduces Smith's (1979) criteria to $Na/U \gg 1$ for propagating waves and $Na/U \ll 1$ for evanescent waves.

Table 1 lists estimated values of N/U for the case studies. The east–west component of the wind speed was evaluated for the midpoint of each layer by assuming a linear profile between the estimated surface gradient wind speed at 300 m (the height of the Darling Scarp) and the height of the critical level, taken as the height at which the shallow surface easterlies turn to the prevailing westerly stream. This table suggests a transition between hydrostatic flows and nonhydrostatic waves at approximately $N/U \sim 0{\cdot}003$ m^{-1}, that is $Na/U \sim 4{\cdot}8$, for the lowest layer, which compares favourably with Klemp and Lilly's (1980) requirement of $Na/U > 10$ for propagating waves dominated by hydrostatic

TABLE 1. ESTIMATED VALUES OF N/U FOR SELECTED LAYERS, WHERE U IS THE EAST–WEST COMPONENT OF THE WIND VELOCITY AT THE MIDPOINT OF THE LAYER AND N IS THE BRUNT–VÄISÄLÄ FREQUENCY

Date	Layers (m)	$d\theta$ (K)	N (s^{-1})	U ($m\ s^{-1}$)	N/U (m^{-1})
3 Feb. 1987	660–865	10·1	0·0405	10·1	0·0040
	865–1550	6·7	0·0180	5·8	0·0031
	1550–2120	1·0	0·0077	0·0	
13 Dec. 1986	738–800	6·3	0·058	13·0	0·0045
	800–1440	5·3	0·0164	10·4	0·0016
	1440–2400	1·4	0·0068	4·5	0·0015
21 Jan. 1987	475–800	0·5	0·007	13·6	0·0005
	800–1730	14·3	0·0225	9·9	0·0023
	1730–2240	4·0	0·016	6·1	0·0026
	2240–2800	0·3	0·004	4·0	0·001
20 Feb. 1987	500–1100	1·2	0·0082	14·6	0·0006
	1100–1240	6·2	0·0385	11·3	0·0034
	1240–2160	8·4	0·0174	7·3	0·0024

effects. Hence for days with similar easterly wind components, the flow can be differentiated by the stability of the lower layer, with stronger stability leading to more dominant hydrostatic effects.

The observations for 3 February suggest that the wave has amplified or developed suddenly, and tend to support the critical-level reflection theory of Clark and Peltier (1984), with resonant amplification observed when the critical level was approximately 0·75 of the wavelength of the vertically propagating wave. Recent modelling studies by Durran and Klemp (1987) question this analysis. Their numerical model suggests that since amplification to wave overturning was not observed, the vertically propagating wave did not meet the requirements to develop into a hydraulic jump. According to Smith and Sun (1987), this occurs when Nh/U, where h is the height of the orography, is small in unidirectional flow, or when the wind reversal is at an improper altitude, in back-sheared flow, leading to a continuous field of vertically propagating waves, rather than a neutral decoupling region and layer-like hydraulic flow. Hence, under this theory, the wind reversal was at the wrong altitude for the development of a hydraulic jump, although it fails to explain the apparent strengthening of the resultant wave. Unfortunately, the current field data are insufficient to clarify this issue.

A hydraulic jump is evident in the observations for 13 December, wherein the upwind conditions approximate the classical requirements of a two-layer hydraulic jump (Long 1954). In particular, there is a sharp inversion to act as a discontinuity, layers above and below which are much less stable and approach neutrality.

On 20 February, the observations show a region of overturning isentropes at 0·5 of the wavelength of the vertically propagating wave, in accord with Lilly and Klemp (1979) for highly asymmetric topography. Further, Lilly and Klemp (1980) suggested that Peltier and Clark's (1979) hypothesis of reflection from a critical level would lead to nonlinear wave suppression rather than amplification, although such a simulation has not been reported.

No catastrophic breakdown of the wave was associated with this overturning but rather we observed a quasi-steady lee wave and extreme turbulence below and to the lee of the overturning. As this feature was observed in both aircraft traverses at this height, it suggests that wave overturning does not destroy the wave. Rather the overturning wave appears to be steady, whilst the quasi-steady nature of the lee waves may result from an oscillation between the degree of overturning and the resultant lee waves. This is consistent with the numerical simulations of Clark and Farley (1984), who observed a periodic build up and then convective breakdown within the overturning wave, resulting in periodic gustiness near the surface.

6. Conclusions

Preliminary observations of forced flow over the Darling Scarp of Western Australia have been presented for four case studies. These illustrate hydraulic jumps, lee waves or vertically propagating hydrostatic waves depending on the upwind stability and wind profile. The observations are for highly asymmetric topography under shallow surface gradient winds wherein a stable layer is formed through nocturnal radiational cooling of the surface. As a result, the mountain halfwidth (of the steeper slope) required to produce propagating hydrostatic waves in these conditions is much smaller than it is for symmetrical topography. Also a consistent wind reversal aloft implies a critical level for the flows. This preliminary analysis suggests that with similar easterly winds, these flows are distinguishable in terms of their upstream temperature profiles, with broad stable layers leading to resonant lee waves whereas with stronger surface inversions buoyancy forces dominate, producing freely propagating waves or hydraulic jumps. These propagating waves and hydraulic jumps are observed to produce accelerated flow down the escarpment.

Acknowledgements

This study has been supported by the Australian Research Grants Scheme and Murdoch University's Special Research Grant. Throughout it, one of the authors (ROP) was in receipt of a Commonwealth Postgraduate Research Award. All aircraft flights were under the command of Mr Phil Butherway. Mr Juri Kuuse and Mr Len Van Burgel of the Commonwealth Bureau of Meteorology provided the radiosonde and anemometer data. The figures were draughted by Mr Allan Rossow, Mr Mike Roeger and Mr Murray Austen-Smith. The paper has also benefited from the comments of an anonymous referee. All of this assistance is gratefully acknowledged.

References

Bower, J. B. and Durran, D. R. 1986 A study of wind profiler data collected upstream during windstorms in Boulder, Colorado. *Mon. Weather Rev.*, **114**, 1491–1500

Clark, T. L. and Farley, R. D. 1984 Severe downslope windstorm calculations in two and three spatial dimensions using anelastic interactive grid nesting: a possible mechanism for gustiness. *J. Atmos. Sci.*, **41**, 329–350

Clark, T. L. and Peltier, W. R. 1977 On the evolution and stability of finite-amplitude mountain waves. *ibid.*, **34**, 1715–1730

1984 Critical level reflection and the resonant growth of nonlinear mountain waves. *ibid.*, **41**, 3122–3134

Corby, G. A. 1957 A preliminary study of atmospheric waves using radiosonde data. *Q. J. R. Meteorol. Soc.*, **83**, 49–60

Durran, D. R. 1986 Another look at downslope windstorms. Part 1: The development of analogs to supercritical flow in an infinitely deep, continuously stratified fluid. *J. Atmos. Sci.*, **43**, 2527–2543

Durran, D. R. and Klemp, J. B. 1987 Another look at downslope winds. Part II: Nonlinear amplification beneath wave-overturning layers. *ibid.*, **44**, 3402–3412

Hoinka, K. P. 1985 Observation of the airflow over the Alps during a foehn event. *Q. J. R. Meteorol. Soc.*, **111**, 199–234

Klemp, J. B. and Lilly, D. K. 1975 The dynamics of wave induced downslope winds. *J. Atmos. Sci.*, **32**, 320–339

1980 'Mountain waves and momentum flux'. Pp. 116–141 in *Orographic effects in planetary flows.* GARP Series No. 23, World Meteorological Organisation

Lester, P. F. and Fingerhut, W. A. 1974 Lower turbulent zones associated with mountain lee waves. *J. Appl. Meteorol.*, **13**, 54–61

Lilly, D. K. and Klemp J. B. 1979 The effects of terrain shape on nonlinear hydrostatic mountain waves. *J. Fluid Mech.*, **95**, 241–261

1980 Comments on 'The evolution and stability of finite-amplitude mountain waves. Part II: Surface wave drag and severe downslope windstorms'. *J. Atmos. Sci.*, **37**, 2119–2121

Lilly, D. K. and Zipser, E. J. 1972 The front range windstorm of 11 January 1972: a meteorological narrative. *Weatherwise*, **25**, 56–63

Long, R. R. 1954 Some aspects of the flow of stratified fluids. II. Experiments with a two-fluid system. *Tellus*, **6**, 97–115

Peltier, W. R. and Clark, T. L. 1979 1980 The evolution and stability of finite-amplitude mountain waves. Part II. Surface wave drag and severe downslope windstorms. *J. Atmos. Sci.*, **36**, 1498–1529 and **37**, 2122–2125

Smith, R. B. 1979 The influence of mountains on the atmosphere. *Adv. Geophys.*, **21**, 87–230

1985 On severe downslope winds. *J. Atmos. Sci.*, **42**, 2598–2603

1987 Aerial observations of the Yugoslavian Bora. *ibid.*, **44**, 269–297

Smith, R. B. and Sun, J. 1987 Generalized hydraulic solution pertaining to severe downslope winds. *ibid.*, **44**, 2934–2939

Tomine, K. 1987 A supplementary study of simulations of mountain wave—critical level interaction. *J. Meteorol. Soc. Jap.*, **65**, 145–149

Vergeiner, I. and Lilly, D. K. 1970 The dynamic structure of lee wave flow as obtained from balloon and airplane observations. *Mon. Weather Rev.*, **98**, 220–232